IEEE Access
Multidisciplinary : Rapid Review : Open Access Journal

Received August 30, 2021, accepted October 19, 2021, date of publication October 22, 2021, date of current version October 28, 2021.

Digital Object Identifier 10.1109/ACCESS.2021.3122379

Fully Integrated THz Schottky Detectors Using Metallic Nanowires as Bridge Contacts

AHID S. HAJO[1], (Member, IEEE), SASCHA PREU[1], (Member, IEEE), LEONID KOCHKUROV[2], THOMAS KUSSEROW[3], AND OKTAY YILMAZOGLU[1]

[1]Department of Electrical Engineering and Information Technology, Institute for Microwave Engineering and Photonics (IMP), Technical University of Darmstadt, 64283 Darmstadt, Germany
[2]Department of Instrumentation Engineering, Saratov State Technical University, 410012 Saratov, Russia
[3]Institute of Nanostructure Technologies and Analytics/CINSaT, University of Kassel, 34132 Kassel, Germany

Corresponding authors: Ahid S. Hajo (ahid.hajo@tu-darmstadt.de) and Oktay Yilmazoglu (oktay.yilmazoglu@tu-darmstadt.de)

This work was supported in part by the German Research Foundation, and in part by the Open Access Publishing Fund of the Technical University of Darmstadt.

ABSTRACT This paper investigates fully integrated Terahertz (THz) Schottky detectors using silver (Ag) metallic nanowires (NWs) with 120 nm diameter as bridge contacts for zero-bias operating THz detectors based on highly doped Gallium Arsenide (GaAs) and Indium Gallium Arsenide (InGaAs) layers. The combination of InGaAs and metallic NWs shows improved performance at zero-bias than a GaAs based detector with a simulated capacitance of 0.5 fF and a series resistance of 29.7 Ω. Thus, the calculated maximum cut-off frequency of 2.6 THz was obtained for a NW contacted vertical InGaAs THz detector. Initial THz measurements were carried out using a common THz setup for frequencies up to 1.2 THz. A responsivity of 0.81 A/W and a low noise-equivalent power (NEP) value of 7 pW/$\sqrt{Hz}$ at 1 THz were estimated using the measured IV-characteristics of the zero-bias NW-InGaAs based THz Schottky detector.

INDEX TERMS Nanowire, Schottky diode, terahertz detector, gallium arsenide, indium gallium arsenide.

I. INTRODUCTION

THz (100 GHz - 10 THz) nanotechnologies represent a new approach to material science and engineering, as well as for design of new devices and processes for the fabrication of compact high-frequency devices. THz detectors, such as Schottky diodes, were intensively investigated in the last 30 years [1]–[3]. Further good and reliable THz detector concepts include complementary metal-oxide-semiconductor (CMOS) [4] and bolometers with some drawbacks. The most sensitive bolometers require a low temperature environment, which increases the cost and the fabrication complexity. CMOS detectors are frequently implemented with resonant antennas in order to tune out the device reactance, limiting the bandwidth [5]. THz Schottky detectors need reliable submicron anode contacts with a low capacitance. For future generations of THz systems, an improvement of the detection sensitivity and system resolution is a must in many applications. In particular, the THz imaging systems suffer from the considerably low power of THz sources as compared to other spectral domains requiring very sensitive detectors. Further potential applications in non-destructive testing of small cell structures in biomedical research, skin cancer detection or in safety engineering can profit from improved detectors. Over the last two decades, tremendous advances have been made in devices ranging from the introduction of new operation concepts to new material choices and improvement in fabrication processes [6]–[12]. Examples of them are High-Electron Mobility Transistors (HEMTs) which use the rectification effect by the Dyakonov-Shur instability. Even HEMTs with much longer gate lengths and cut-off frequencies in the GHz range enable detection of THz waves [13].

To date, Schottky diodes are still the most sensitive detector concept for direct detection of THz radiation at room temperature. This kind of detector combines a high responsivity with very short response time and compact dimensions. It shows excellent performance in the sub-mm wavelength range. The output signal is proportional to the incoming power over a wide range of powers. AC-coupled Schottky receivers can measure the field intensity of individual terahertz pulses [14], [15]. Nagatsuma *et al.* used a Schottky receiver to build a wireless communication system towards 100 Gbit/s at 100 GHz [16]. Typically, the best performance at room-temperature conditions can be achieved for waveguide-coupled Schottky diode detectors with responsivities ranging from 4000 V/W at 100 GHz to about 400 V/W at 900 GHz

The associate editor coordinating the review of this manuscript and approving it for publication was Jenny Mahoney.

This work is licensed under a Creative Commons Attribution 4.0 License. For more information, see https://creativecommons.org/licenses/by/4.0/

and the minimum NEP of about 1 pW/ $\sqrt{Hz}$ at 100 GHz [2]. However, the frequency bandwidth of waveguide-based detectors is limited by the physical size, whereas for many applications such as THz spectroscopy, it is highly desirable to achieve wider operating bandwidths going to more broadband radiation coupling schemes [17]. In combination with fast response time this contributes to the emergence of new application areas [26]. The low NEP of Schottky detectors can allow the passive detection of low power down to black body radiation. It was also shown that alternative rectifier methods based on InP/InGaAs heterostructures [18] with Fermi-level managed barriers and heterojunction low barrier diode based on AlGaInAs [19] can be used for low noise, low-level radiometric detection with a responsivity of 1110 V/W at 300 GHz and 1700 V/W at 220 GHz, respectively. Ito and Nadar achieved a NEP of $\sim$ 1.3 pW/ $\sqrt{Hz}$ at 200 GHz and 3 pW/ $\sqrt{Hz}$ at 300 GHz, respectively. Other publications have shown a modified Schottky barrier height on semiconductors due to reduced Fermi-Level pinning with nanoparticles from few nanometer to > 20 nm [3]. Similar to this approach, our metallic nanowires reduce the Schottky barrier height. This property and the low capacitance lead to efficient zero-bias operation and low noise THz detection capability.

In this contribution, the conventional Schottky contact was replaced with a NW to achieve a new Schottky diode for THz detection. The use and further investigation of these emerging and extremely demanding concepts with metallic NWs on semiconducting mesas (SC-Mesa) constitute the significant novelty of this work over earlier efforts in the field with standard contacts [5]. The new devices have benefits besides the reduction of the fabrication complexity (no need for high resolution lithography for small contact in nanometer range, like electron-beam lithography), enhanced electric field at the Schottky contact with reduced Schottky barrier height [20]–[24]. Furthermore, NWs can be aligned using several methods: for example by nanostructure grooves [25], with nano-tweezers [26] or using the dielectrophoresis (DEP) technique [27]. In this work, the metallic NWs were aligned using DEP. These THz Schottky detectors based on GaAs and InGaAs were simulated, fabricated and characterised using Ag-NWs with 120 nm diameter as bridge contacts and were compared to standard detectors (SD) fabricated with evaporated finger contacts.

II. SIMULATIONS

The device capacitances were simulated for different configurations using CST EM Studio. In the CST simulation, a NW with a diameter of 120 nm and a contact length of 2 μm was used for the capacitance calculation. The mesa has a width of 7 μm and a length of 4 μm and contents of two layers. The bottom layer has a height of $[1]\mu m$ with $n^{++} = 5 \cdot 10^{18} cm^{-3}$ and the top layer has the height of $[0.1]\mu m$ with $n^{+} = 1 \cdot 10^{18} cm^{-3}$, respectively. The thickness of the antenna arms (Ant 1 and Ant 2, Fig. 1) and the ohmic contact was 120 nm. The parameters were set using CST EM Studio environment which can simulate the

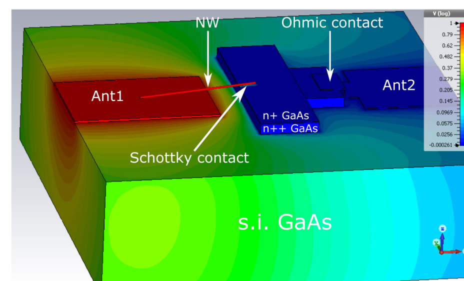

FIGURE 1. CST simulation of the potential distribution of the GaAs Schottky diode using silver NW as air-bridge contact. Ant1 and Ant2 are the inner parts of both antenna arms that were connected to the Schottky diode. The same configuration was also used for the InGaAs diode. The total simulated capacitance of both devices was 0.5 fF.

potential distribution of the device. The electrostatic solver was used which can provide the capacitance of the module. The capacitance of the NW and of the SD based diodes was simulated as 0.5 fF and 2 fF, respectively, which can be used to determine the maximum cut-off frequencies. Figure 1 shows the CST simulation results of the potential distribution, from which the capacitance was calculated. The simulated capacitance of the InGaAs diode was almost equal to the simulated capacitance of the GaAs diode due to the same geometry.

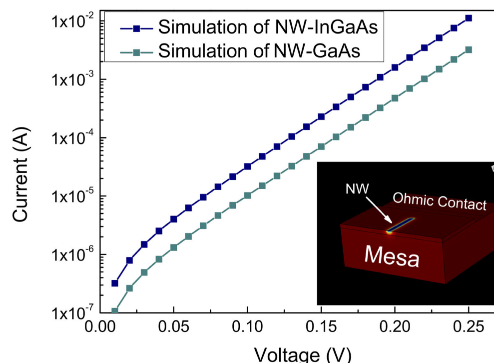

FIGURE 2. Simulated IV-characteristics of GaAs and InGaAs based Schottky diodes using COMSOL. The inset indicate the modelled device.

Furthermore, numerical modelling of the device was performed using COMSOL Multiphysics. For the COMSOL simulation, the semiconductor module was used as a setting environment at a temperature of 300 K. The model under study (inset of Fig. 2) consists of two sandwiched n-doped layers of GaAs or InGaAs with the same thicknesses and doping concentrations used in the CST simulation. The impurity concentration of the semiconductor material was set in the doping module for the Schottky contact. A Ag-NW was placed on the top of the semiconductor structure as Schottky contact with an estimated width and length of 30 nm (only the bottom curvature of the NW was used) and 2 μm, respectively. Then, a voltage between 0 V and 1 V was applied. This sweep voltage was set in the auxiliary sweep under study/stationary. Figure 2 represents the simulated IV curve obtained with our model.

III. FABRICATION AND RESULTS

In order to investigate the room temperature THz detectors, four detector types were fabricated: Two detectors were based on standard contacts and the other two were based on Ag-NW contacts. A small NW diameter of 120 nm was used to have better contact in comparison to a thicker NW because of its mechanical flexibility on the active layer. The finger contact was evaporated using Ti/Au (20 nm/120 nm) with a finger width of 1 μm and a length of 2 μm. All detectors were fabricated with highly doped epitaxial layers with the same material configurations mentioned in the simulation part. The semi-insulating (s.i.) substrates have a thickness of 300 μm (s.i.-GaAs for n-GaAs, s.i.-InP for n-InGaAs). Figure 3 (a) illustrates the diode RF equivalent circuit used to calculate the power lost due to the impedance mismatch of the device and the antenna and (b) the 3D close-up of device structures. The ohmic contact of the diodes was fabricated with Ni/AuGe/Ni and annealed at 420°C. A silicon dioxide (SiO_2) passivation layer under the antenna is used to avoid any leakage current. The antenna metallization is made of Ti/Au with thickness of 20 nm and 120 nm, respectively. Afterwards, an additional passivation layer was deposited on top to prevent any short circuit of the antenna with the aligned NWs. Only the part between the mesa and one antenna arm was opened to contact the Schottky diode with the NW.

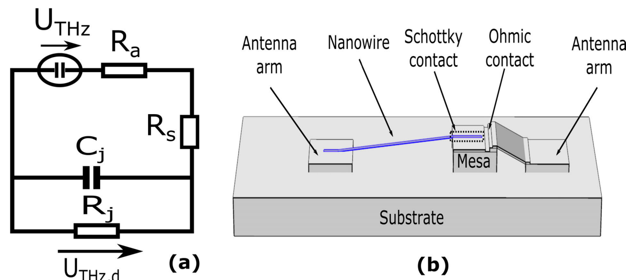

FIGURE 3. (a) Diode RF equivalent circuit used to calculate the power losses (b) 3D close-up of the Schottky detector using the nanowire as a bridge and anode contact.

DEP was then used for the selective alignment. The DEP uses an AC electric field to manipulate neutrally charged particles in a solution and offers a promising method to attract NWs onto predefined electrodes. The process parameters depend on the volume, length and material of the NWs. A potential of 2 Vp-p with a square-wave and a frequency of 30 kHz was applied to align the NW. The NW diameter and the controlled alignment determine the junction and parasitic capacitance as well as the series resistance. Figure 4 shows the SEM images of the Schottky contacts using DEP technique. Figure 4 (a) illustrates a single Ag-NW. In Fig. 4 (b), a NW was contacted with a part of an antenna. A comparison between aligned single NW Fig. 4 (c) and multi-NWs as a multi-finger Schottky contact Fig. 4 (d) are also shown for selective alignments using DEP.

Figure 5 shows a SEM image of the fabricated detector with an aligned NW in the middle of the antenna structure.

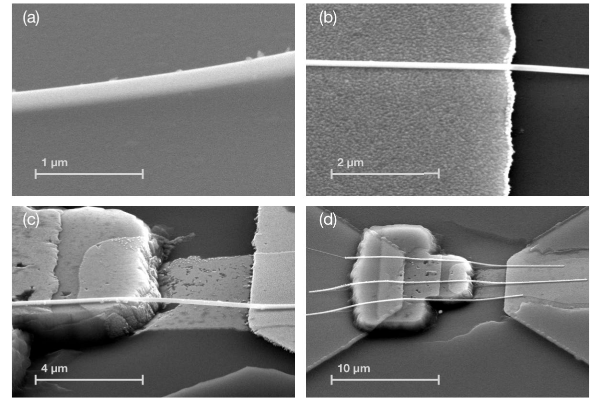

FIGURE 4. SEM images of the Schottky contacts using DEP technique. (a) Single Ag-NW. (b) NW contacted with one arm of the antenna. A comparison between aligned single NW (c) and multi-NWs as a multi-finger Schottky contact (d). A part of the integrated antenna is also shown in (d).

All other NWs have no influence due to surface passivation. These NWs are leftovers of the process due to the use of the DEP. The alignment of the DEP technique is accurate to contact many NWs in a small area. On one hand however, the NWs are in suspension and this medium contains tens of NWs per device area which makes the alignment of a single NW difficult, therefore few NWs are spread together on the whole structure. On the other hand, the DEP force depends on the fluid flow and the interaction between the NW and the surfaces around which impaired the accuracy of this method. An alignment accuracy of 500 nm was achieved in the way that several NWs lie side by side without causing a short circuit.

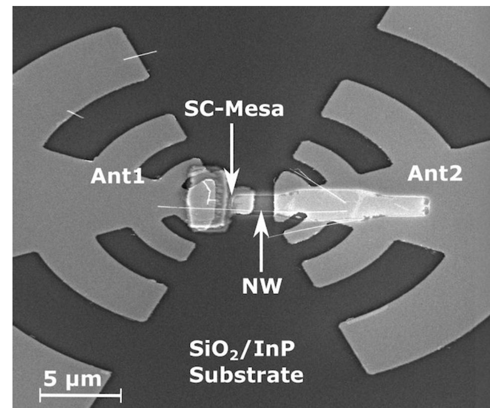

FIGURE 5. SEM image of the fabricated Schottky detector with a log-periodic broadband THz antenna. The NW has a diameter of 120 nm.

A. IV-CHARACTERISTICS OF THE DIODES

First of all, both SD-GaAs and NW-GaAs based detectors were characterized. Figure 6 shows the IV-characteristics of these diodes. In addition, we changed the active material to InGaAs because of its higher electron mobility, smaller band gap and smaller Schottky barrier height. The SD-InGaAs

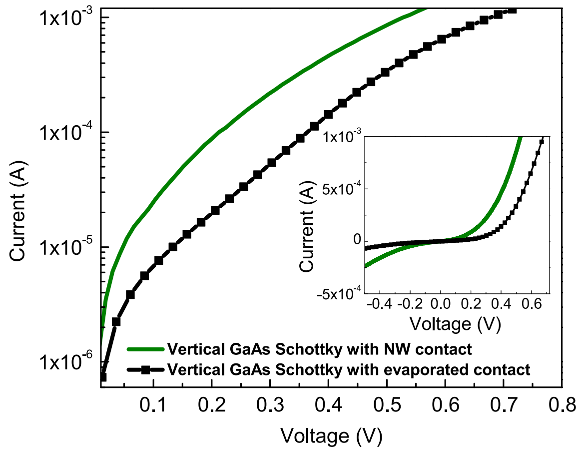

FIGURE 6. A comparison of the IV-characteristics between the vertical NW-GaAs and the SD-GaAs Schottky detectors. The inset indicates the linear IV-characteristic of the same diodes.

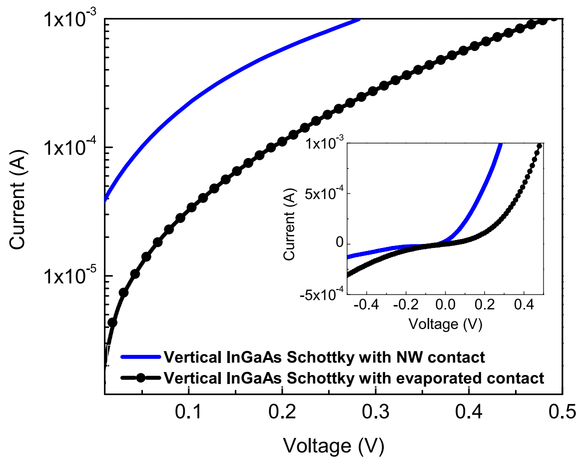

FIGURE 7. A comparison of the IV-characteristics between the vertical NW-InGaAs and the SD-InGaAs based Schottky detectors. The inset shows the linear IV-characteristic of the same diodes.

and NW-InGaAs based detectors were characterized as well (Fig. 7). Figure 8 shows a comparison of the NW-GaAs and the NW-InGaAs based detectors. The NW-based devices were characterised with one single NW with a diameter of 120 nm.

Similar to Casini *et al.* [3], the metallic NW increases the electrical field at the Schottky contact to achieve higher current at lower voltage than the standard Schottky diode with evaporated contact. A parasitic thin oxide layer under the Schottky contact is less critical for the NW due to the field enhancement. The modification at the forward bias with relatively high current density creates an effective channel, unlike for the evaporated contact. This shows that a semiconductor surface treatment is not as critical as for the evaporated Schottky contact. Unlike the simulated structure which has a contact length of 2 μm, the fabricated diodes have an estimated contact length of $< 1\ \mu m$ due to the bending of the NW and the passivation layer (to protect a short circuit between

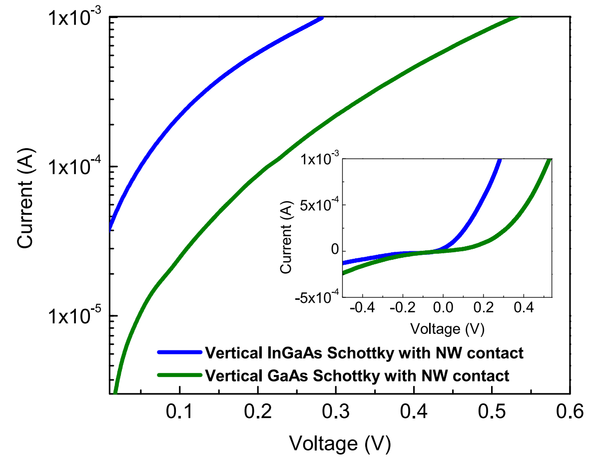

FIGURE 8. A comparison of the IV-characteristics between the vertical InGaAs and the GaAs based Schottky detectors. Both detectors are based on NW contacts with 120 nm diameter. The inset shows the linear IV-characteristics of the same diodes.

the NW and the ohmic contact), so the lowermost part of the NW curvature does not contact the active material well. Therefore, the forward current is smaller for the fabricated devices. Generally, the simulations show an ideal scenario, therefore the results look better. There is probably still 0.5 fF of parasitic capacitance in the system, which is not captured by the simulation. In the future, the NW will be aligned closer to the designed structure as the simulation shows to achieve a longer contact on the mesa for a higher current.

B. EXTRACTION OF DIODE PARAMETERS

The resulting DC IV-characteristics show typical diode shapes of the thermionic emission model given by

$$I = A_{eff} A^* T^2 e^{\left(\frac{-q\phi}{k_B T}\right)} \cdot \left(e^{\left(\frac{qV}{nk_B T}\right)} - 1 \right), \tag{1}$$

with the magnitude of electron charge q, the Boltzmann constant k_B and absolute temperature T of 300 K. A^* indicates the Richardson constant of [8.6] $cm^{-2}K^{-2}A$. The series resistances R_s, the barrier height ϕ, and the ideality factor n of both detectors were extracted using the Cheung method [28]. This method enables the determination of the Schottky diode parameters from a single forward bias IV-characteristic at a certain temperature. From equation (2) we get equations (3) and (4)

$$V = R_s \cdot I + n \cdot \phi + \left(\frac{n}{\beta}\right) \cdot \, ln\left(\frac{I}{A_{eff} A^* \cdot T^2}\right), \tag{2}$$

$$\frac{d(V)}{d(\,lnI)} = R_s \cdot I + \frac{n}{\beta}, \tag{3}$$

$$H(I) = R_s \cdot I + n \cdot \phi, \tag{4}$$

where $\beta = q/k_B T$. The plot between $\frac{d(V)}{d(\,lnI)}$ and the current I gives a straight line ($y = ax + b$), where R_s can be indicated from the slope and the y-intercept of this plot

provides the n value. The intercept of the linear fit of the plot between $H(I)$ and I gives ϕ. We have extracted different diodes and found out that n was about 1.2 - 1.49. These different values are attributable to the varying alignments of the Schottky contacts. In comparison to the extracted barrier height using the thermionic emission model found in the literature as 0.56 eV [29] and 0.24 eV [30] for the SD-GaAs and SD-InGaAs, respectively, the lowest determined effective barrier height according to equation (5) for our NW-GaAs and NW-InGaAs based diodes was 0.4 eV and 0.21 eV

$$\phi = \frac{k_B T}{q} \, ln \left(\frac{A_{eff} A^* T^2}{I_s} \right), \tag{5}$$

with the saturation current I_s. The saturation current was about 1 nA and 138 nA for NW-GaAs and NW-InGaAs, respectively. The enhanced electrical fields for the NW based diodes can decrease the Schottky barrier height related to the image-force barrier lowering [31]. The effective area A_{eff} was defined as an approximation of $6 \cdot 10^{-10}$ cm^2 because only the lowermost part of the NW curvature [width 30 nm times length 2 μm] under the NW was considered as contact area.

From Sze *et al.* [32], the Schottky junction capacitance was calculated as $C_j = 0.48$ fF, which fits with our simulated one of 0.5 fF. Using this value of the junction capacitance and the series resistance R_s of 29,7 Ω (with an error of ±30%) in $f_{cut-off}^{max} = 1/(2\pi C_j R_s)$, we estimate a maximum cut-off frequency of 10.7 THz for the vertical contacted NW-InGaAs diode. However, the junction resistance R_j and antenna resistance R_a influence the actual cut-off frequency. Using equation (6) [33]

$$f_{cut-off} = \frac{1}{2\pi R_j C_j} \sqrt{\frac{R_s + R_a + R_j}{R_s + R_a}}, \tag{6}$$

the calculated cut-off frequency for the vertical contacted NW-InGaAs diode at zero-bias operation is obtained as 1.7 THz with $C_j = 0.5$ fF, $R_j = 420\,\Omega$, $R_a = 70\,\Omega$ and $R_s = 29.7\,\Omega$, where R_a is the average radiation resistance of the logarithmic-periodic antenna according to simulations. For the same diode at near zero-bias operation at 0.1 V, a cut-off frequency of 2.6 THz is expected with $C_j = 0.5$ fF, $R_j = 214\,\Omega$, $R_a = 70\,\Omega$ and $R_s = 29.7\,\Omega$. This is due to the decreased R_j with increased bias voltage.

At frequencies greater than 1 THz, the frequency-dependent skin effect should be taken into account [34] due to the increase of the series resistance which in turn reduces the cut-off frequency. In the Schottky diode, the skin effect δ occurs in the metallic NW and in the semiconductor buffer layer. The skin depth can be described as follows [34], [35]

$$\delta = \sqrt{\frac{2}{\omega \cdot \mu_{(NW)} \cdot \sigma_{(NW)}}}, \tag{7}$$

where ω is the radial frequency, μ the permeability and σ the conductivity of the NW. For Ag-NWs at a frequency of 1 THz, the skin depth is 63.42 nm. Therefore a NW diameter of 120 nm was used to avoid the skin effect. This means at frequencies higher than 1 THz, a part of the NW is free from the AC currents.

C. THz RESPONSIVITY AND NEP

In order to highlight the peculiarity of these devices, a comparison of the quasi-DC responsivity (the numerical second derivative of the IV curve) was performed for all detectors (Fig. 9), which is a direct indicator for the responsivity. This method was also used in [36] and showed an accurate agreement with the measured responsivity. Thus, it is useful to look at the quasi-DC responsivity as a function of the DC bias voltage hence as long the detected current I_{THz}^{DC} is in the small signal limit proportional to the second derivative of the IV curve. Consequently, the theoretical responsivity $\Re$ can be estimated by

$$\Re(A/W) = R_a \cdot \frac{d^2 I}{dV^2} \, |_{V_{DC}} \; \eta_{tot}, \tag{8}$$

where η_{tot} contains all losses, including the impedance mismatch of the antenna and the device η_{imp}

$$\eta_{imp} = \frac{R_j || C_j}{(R_j || C_j) + (R_s + R_a)}, \tag{9}$$

calculated using the equivalent circuit shown in Fig. 3 (a), as well as the optical losses η_{opt} at the interface of the silicon lens and air.

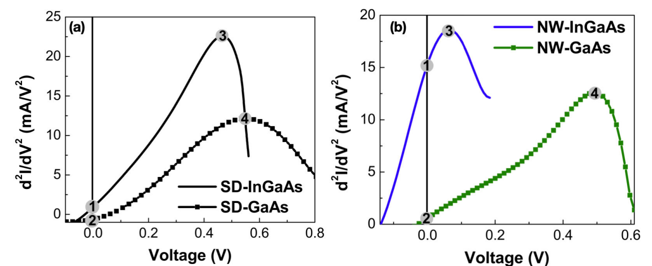

FIGURE 9. A comparison of the quasi-static DC responsivities between the vertical SD-GaAs and SD-InGaAs (a) as well the NW-GaAs and NW-InGaAs (b) based Schottky detectors.

The relative comparison between our SDs with an evaporated contact (Fig. 9 (a)) shows that the SD-InGaAs based Schottky diodes have lightly higher responsivity at zero-bias operation than the SD-GaAs based Schottky diodes and a higher quasi-DC responsivity with a factor of about 2 at 0.45 V (operation points 3 and 4). Moreover, the detector based on NW-InGaAs has significantly higher responsivity under zero-bias operation than the NW-GaAs with a factor of about 15 (Fig. 9 (b) point 1 and 2). Therefore the NW-InGaAs was used to reduce the noise floor and the complexity of the setup for zero-bias THz detection. At this point of operation, the NW-InGaAs indicates a maximum possible responsivity of $\Re = 15\,mA/V^2 \cdot R_a = 1.08$ A/W. Using equation (8) with the impedance losses η_{imp} of approximately 25%, we expect a responsivity of 0.81 A/W and a low NEP value of 7 pW/$\sqrt{Hz}$ at 1 THz using the measured

IV-characteristic of the NW-InGaAs based THz Schottky detector. The NEP value was calculated by

$$NEP = \frac{\sqrt{4k_BT/(R_s + R_j)}}{\Re}. \quad (10)$$

Note that the losses of approximately 25% were calculated without taking the optical losses η_{opt} into account.

D. THz MEASUREMENTS

A common THz setup with a LTG-GaAs lateral photomixer with conventional interdigital fingers was used [37], [38]. The THz beam was generated by using two tunable distributed feedback laser (DFB) with a wavelength of about 850 nm which were coupled by a 50:50 combiner. An optical laser power of the beat signal of 20 mW was focused onto the active region of the photomixer employing a polarization-maintaining optical fiber. To accelerate the generated carrier, a DC potential of up to 12 V was applied. The photomixer was mounted on a hyper-hemispherical Si lens to couple and direct the THz radiation into two parabolic mirrors which in turn direct the THz beam to the Schottky detector. The dark current and the photocurrent were measured as 200 nA and 1.0 mA at 12 V, respectively. Commercial transimpedance amplifier and Lock-in technique for noise suppression were used to measure the relative THz signal. A Golay cell as a reference for the THz Schottky detector measurements was used.

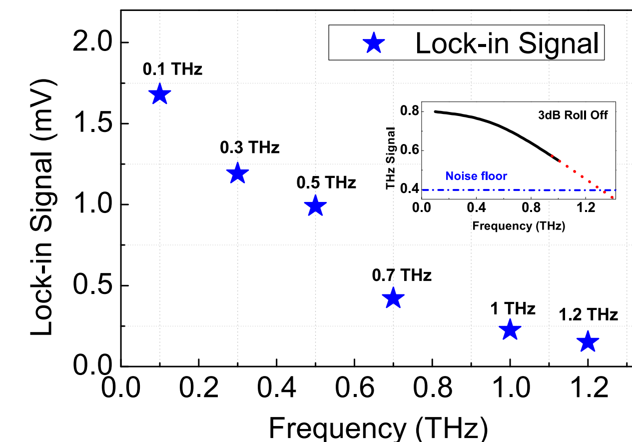

FIGURE 10. THz measurements using NW-InGaAs based Schottky detector at zero-bias operation. The maximum measured frequency was about 1.2 THz, this is due to the limitation of the used photomixer. The inset refers to the extrapolated RC Roll-off of about 1.2 THz.

The initial THz measurement was carried out using the zero-biased NW-InGaAs based Schottky detector (Fig. 10). The THz detector was measured at 100 GHz, 300 GHz, 500 GHz, 700 GHz, 1.0 THz and 1.2 THz and showed an output voltage of 0.15-1.69 mV. The used photomixer was limited to about 1.2 THz. These measurements are still initial and need optimizations on one hand on the source side and on the other hand on the detector side as well.

In Table 1, a comparison of the cut-off frequency and NEP value of the NW-InGaAs based Schottky detector compared to the state-of-the-art results is given. The Schottky diode with a curvature contact presented in [3] operates at 550 GHz with a NEP of 0.5 nW/$\sqrt{Hz}$ and needs an electron-beam lithography. With the Fermi-level managed barrier Schottky diode [18] and a heterojunction low barrier AlGaInAs based Schottky diode [19], a NEP of 3 pW/$\sqrt{Hz}$ at 0.3 GHz and 1.3 pW/$\sqrt{Hz}$ at 0.2 THz was achieved, respectively. The CNT (carbon nanotube) based Schottky diode with a NEP of 0.1 pW/$\sqrt{Hz}$ at 0.6 GHz presented in [33] uses the CNT as an active material but it includes only the diode without antenna, so the manufacture constraints for THz frequencies were only modelled. Another device based on phosphorus implanted Schottky diode on graphene/SiC presented in [36] shows an estimated NEP of 5 pW/$\sqrt{Hz}$ at $\approx$ 90 GHz (limited by the RC circuitry). A Schottky diode with a standard evaporated contact presented in [39] reaches a frequency of about 0.8 THz with a NEP of 10 pW/$\sqrt{Hz}$. Further low Barrier Schottky diode with standard contact found in [40] has a NEP of 0.39 pW/$\sqrt{Hz}$ at $\approx$ 90 GHz. The vertical NW-InGaAs based Schottky detector presented in this work reaches frequencies up to 1.2 THz (limited by the used source) with an estimated NEP of 7 pW/$\sqrt{Hz}$ at 1 THz.

TABLE 1. The cut-off frequency and NEP value of NW-InGaAs based Schottky detector compared to the state-of-the-art results.

Device | Parameter	NEP (W/$\sqrt{\text{Hz}}$)	$f_{\text{cut-off}}$ (THz)
Vertical NW-InGaAs Schottky diode (this work)	$7{\cdot}10^{-12}$ @ 1 THz	2.6 (Estimated); 1.2 (Measured)
GaAs based Schottky diode with a curvature contact [3]	$5{\cdot}10^{-10}$ @ 0.55 THz	0.55 (Measured)
Fermi-level managed barrier InGaAs Schottky diode [18]	$3{\cdot}10^{-12}$ @ 0.3 THz	1.0 (Measured)
Heterojunction low barrier AlGaInAs Schottky diode [19]	$1.3{\cdot}10^{-12}$ @ 0.2 THz	0.2 (Measured)
CNT Schottky diode [33]	$0.1{\cdot}10^{-12}$ @ 0.8 THz	2.5 (Estimated)
Phosphorus implanted Schottky diode on graphene/SiC [36]	$5{\cdot}10^{-12}$ @ 0.09 THz	0.1 (Measured)
InGaAs Schottky diode with standard contact [39]	$10{\cdot}10^{-12}$ @ 0.1 THz	2.0 (Estimated); 0.8 (Measured)
Low Barrier InGaAs Schottky diode with standard contact [40]	$0.39{\cdot}10^{-12}$ @ $\approx$ 0.09 THz	0.2 (Measured)

IV. CONCLUSION

In this paper, a metallic NW configuration was used for THz Schottky detectors. The vertical NW-InGaAs Schottky detector showed much higher zero bias responsivity in comparison to the detector based on NW-GaAs and thus to the SDs. Both Schottky detectors were fabricated on n+GaAs or on n+InGaAs structure using the NW as bridge-contact on the semiconductor mesa. The alignment with dielectrophoresis with an alignment accuracy of 500 nm was applied to contact the NW based Schottky diodes. The simulated capacitance of the device was 0.5 fF which was used to calculate the cut-off frequency of about 2.6 THz. Several initial THz measurements up to 1.2 THz were carried out using a common

THz setup. The detectors work at room temperature and achieved zero-bias operation. A responsivity of 0.81 A/W and a low NEP value of 7 pW/$\sqrt{Hz}$ at 1 THz were estimated using the measured IV-characteristics of the NW-InGaAs based THz Schottky detector. THz detector devices based on dielectrophoretically aligned metallic NWs on low permittivity substrates can result in low cost, room temperature detector operation with high cut-off frequency. Thus, this nano-micro integrated THz detector is promising to fabricate highly sensitive, high frequency imaging and spectroscopy systems for material inspection, security and biomedical applications.

ACKNOWLEDGMENT

The authors would like to thank Computer Simulation Technology (CST) and COMSOL Multiphysics for providing the softwares used for the simulations. Leonid Kochkurov has partly contributed in the COMSOL simulation.

REFERENCES

[1] H. P. Röser, H. W. Hübers, T. W. Crowe, and W. C. B. Peatman, "Nanostructure GaAs Schottky diodes for far-infrared heterodyne receivers," *Infr. Phys. Technol.*, vol. 35, nos. 2–3, pp. 451–462, Mar. 1994.

[2] J. L. Hesler and T. W. Crowe, "Responsivity and noise measurements of zero-bias Schottky diode detectors," in *Proc. 18th Int. Symp. Space THz Technol.*, Pasadena, CA, USA, Mar. 2007, pp. 1–4.

[3] R. Casini, A. Di Gaspare, E. Giovine, A. Notargiacomo, M. Ortolani, and V. Foglietti, "Three-dimensional shaping of sub-micron GaAs Schottky junctions for zero-bias terahertz rectification," *Appl. Phys. Lett.*, vol. 99, no. 26, Dec. 2011, Art. no. 263505.

[4] S. Boppel, A. Lisauskas, V. Krozer, and H. G. Roskos, "Towards monolithically integrated CMOS cameras for active imaging with 600 GHz radiation," *Proc. SPIE*, vol. 8261, Feb. 2012, Art. no. 826106.

[5] R. A. Lewis, "A review of terahertz detectors," *J. Phys. D, Appl. Phys.*, vol. 52, Aug. 2019, Art. no. 433001.

[6] D. Suzuki, S. Oda, and U. Kawano, "A flexible and wearable terahertz scanner," *Nature Photon.*, vol. 10, pp. 809–813, Nov. 2016.

[7] M. Egard, S. Johansson, A.-C. Johansson, K.-M. Persson, A. W. Dey, B. M. Borg, C. Thelander, L.-E. Wernersson, and E. Lind, "Vertical InAs nanowire wrap gate transistors with $f_t > 7$ GHz and $f_{max} > 20$ GHz," *Nano Lett.*, vol. 10, no. 3, pp. 809–812, Mar. 2010.

[8] F. Schwierz, "Graphene transistors," *Nature Nanotechnol.*, vol. 5, no. 7, pp. 487–496, May 2010.

[9] K. Takei, M. Madsen, H. Fang, R. Kapadia, S. Chuang, H. S. Kim, C.-H. Liu, E. Plis, J. Nah, S. Krishna, and Y. L. Chueh, "Nanoscale InGaSb heterostructure membranes on Si substrates for high hole mobility transistors," *Nano Lett.*, vol. 12, no. 4, pp. 2060–2066, 2012.

[10] C. Wang, J.-C. Chien, H. Fang, K. Takei, J. Nah, E. Plis, S. Krishna, A. M. Niknejad, and A. Javey, "Self-aligned, extremely high frequency III–V metal-oxide-semiconductor field-effect transistors on rigid and flexible substrates," *Nano Lett.*, vol. 12, no. 8, pp. 4140–4145, Aug. 2012.

[11] S. Kono, M. Tani, P. Gu, and K. Sakai, "Detection of up to 20 THz with a low-temperature-grown GaAs photoconductive antenna gated with 15 fs light pulses," *Appl. Phys. Lett.*, vol. 77, no. 25, pp. 4104–4106, Dec. 2000.

[12] W. R. Deal, K. Leong, W. Yoshida, A. Zamora, and X. B. Mei, "InP HEMT integrated circuits operating above 1,000 GHz," in *IEDM Tech. Dig.*, Dec. 2016, pp. 29.1.1–29.1.4.

[13] S. Preu, S. Kim, R. Verma, P. G. Burke, M. S. Sherwin, and A. C. Gossard, "An improved model for non-resonant terahertz detection in field-effect transistors," *J. Appl. Phys.*, vol. 111, no. 2, Jan. 2012, Art. no. 024502.

[14] A. Semenov, O. Cojocari, H.-W. Hübers, F. Song, A. Klushin, and A.-S. Müller, "Application of zero-bias quasi-optical Schottky-diode detectors for monitoring short-pulse and weak terahertz radiation," *IEEE Electron Device Lett.*, vol. 31, no. 7, pp. 674–676, Jul. 2010.

[15] F. Rettich, N. Vieweg, O. Cojocari, and A. Deninger, "Field intensity detection of individual terahertz pulses at 80 MHz repetition rate," *J. Infr., Millim., THz Waves*, vol. 36, no. 7, pp. 607–612, Jul. 2015.

[16] T. Nagatsuma, S. Horiguchi, Y. Minamikata, Y. Yoshimizu, S. Hisatake, S. Kuwano, N. Yoshimoto, J. Terada, and H. Takahashi, "Terahertz wireless communications based on photonics technologies," *Opt. Exp.*, vol. 21, nos. 20, pp. 23736–23747, Sep. 2013.

[17] C. Sydlo, O. Cojocari, D. Schçnherr, T. Goebel, P. Meissner, and H. L. Hartnagel, "Fast THz detectors based on InGaAs Schottky diodes," *Frequenz*, vol. 62, nos. 5–6, pp. 107–110, Jun. 2008.

[18] H. Ito and T. Ishibashi, "InP/InGaAs fermi-level managed barrier diode for broadband and low-noise terahertz-wave detection," *Jpn. J. Appl. Phys.*, vol. 56, no. 1, Jan. 2017, Art. no. 014101.

[19] S. Nadar, M. Zaknoune, X. Wallart, C. Coinon, E. Peytavit, G. Ducournau, F. Gamand, M. Thirault, M. Werquin, S. Jonniau, N. Thouvenin, C. Gaquiere, N. Vellas, and J.-F. Lampin, "Sub-THz zero-bias detector with high performances based on heterostructure low barrier diode (HLBD)," in *Proc. 41st Int. Conf. Infr., Millim., THz waves (IRMMW-THz)*, Copenhagen, Denmark, Sep. 2016, pp. 1–2.

[20] A. S. Hajo, S. Al-Daffaie, O. Yilmazoglu, M. T. Haidar, and F. Kuppers, "Zero-bias Schottky diode based THz detectors at room temperature using metallic nanowire," in *Proc. 41st Int. Conf. Infr., Millim., THz waves (IRMMW-THz)*, Copenhagen, Denmark, Sep. 2016, pp. 1–2.

[21] A. S. Hajo, O. Yilmazoglu, and F. Kuppers, "Vertical nanowire contacted THz Schottky detectors based on gallium arsenide for zero-bias operation," in *Proc. 42nd Int. Conf. Infr., Millim., THz Waves (IRMMW-THz)*, Cancun, Mexico, Aug. 2017, pp. 1–2.

[22] A. S. Hajo, O. Yilmazoglu, and F. Kuppers, "New InGaAs THz Schottky detectors with nanowire contact for zero-bias operation," in *Proc. 43rd Int. Conf. Infr., Millim., THz Waves (IRMMW-THz)*, Nagoya, Japan, Sep. 2018, pp. 1–2.

[23] A. S. Hajo, O. Yilmazoglu, S. Lu, F. Kuppers, and T. Kussorow, "Comparison of metallic NW and evaporated contact for THz detector modules based on an InGaAs Schottky diode," in *Proc. 44th Int. Conf. Infr., Millim., THz Waves (IRMMW-THz)*, Paris, France, Sep. 2019, pp. 1–2.

[24] A. S. Hajo, O. Yilmazoglu, F. Kuppers, and T. Kusserow, "Integration and characterisation of Schottky diodes with a pre-amplifier for THz applications," in *Proc. 45th Int. Conf. Infr., Millim., Terahertz Waves (IRMMW-THz)*, Nagoya, Japan, Nov. 2020, pp. 1–2.

[25] H. Wu, Y. Jiao, C. Zhang, C. Chen, L. Yang, J. Li, J. Ni, Y. Zhang, C. Li, Y. Zhang, S. Jiang, S. Zhu, Y. Hu, D. Wu, and J. Chu, "Large area metal micro-/nano-groove arrays with both structural color and anisotropic wetting fabricated by one-step focused laser interference lithography," *Nanoscale*, vol. 11, no. 11, pp. 4803–4810, Mar. 2019.

[26] P. Kim and C. M. Lieber, "Nanotube nanotweezers," *Science*, vol. 286, no. 5447, pp. 2148–2150, Dec. 1999.

[27] J. J. Boote and S. D. Evans, "Dielectrophoretic manipulation and electrical characterization of gold nanowires," *Nanotechnology*, vol. 16, no. 9, pp. 1500–1505, Sep. 2005.

[28] S. K. Cheung and N. W. Cheung, "Extraction of Schottky diode parameters from forward current-voltage characteristics," *Appl. Phys. Lett.*, vol. 49, no. 2, pp. 85–87, Jul. 1986.

[29] T. U. Kampen, S. Park, and D. R. T. Zahn, "Barrier height engineering of Ag/GaAs(100) Schottky contacts by a thin organic interlayer," *Appl. Surf. Sci.*, vol. 190, nos. 1–4, pp. 461–466, May 2002.

[30] S. Mehari, A. Gavrilov, S. Cohen, P. Shekhter, M. Eizenberg, and D. Ritter, "Measurement of the Schottky barrier height between ni-InGaAs alloy and $In_{0.53}Ga_{0.47}As$," *Appl. Phys. Lett.*, vol. 101, no. 7, Aug. 2012, Art. no. 072103.

[31] E. H. Rhoderick, *Metal-Semiconductor Contacts*, 2nd ed. New York, NY, USA: Oxford Univ. Press, 1982.

[32] S. M. Sze, Y. Li, and K. K. Ng, *Physics of Semiconductor Devices*. Hoboken, NJ, USA: Wiley, 2006.

[33] H. M. Manohara, E. W. Wong, E. Schlecht, B. D. Hunt, and P. H. Siegel, "Carbon nanotube Schottky diodes using Ti−Schottky and Pt−ohmic contacts for high frequency applications," *Nano Lett.*, vol. 5, no. 7, pp. 1469–1474, Jul. 2005.

[34] A. Y. Tang and J. Stake, "Impact of eddy currents and crowding effects on high-frequency losses in planar Schottky diodes," *IEEE Trans. Electron Devices*, vol. 58, no. 10, pp. 3260–3269, Oct. 2011.

[35] M. Greconici, G. Madescu, and M. Mot, "Skin effect analysis in a free space conductor," *Facta Universitatis Electron. Energetics*, vol. 23, no. 2, pp. 207–215, Jan. 2010.

[36] M. T. Schlecht, S. Preu, S. Malzer, and H. B. Weber, "An efficient terahertz rectifier on the graphene/SiC materials platform," *Sci. Rep.*, vol. 9, no. 1, pp. 1–8, Dec. 2019.

[37] M. T. Haidar, S. Al-Daffaie, O. Yilmazoglu, A. S. Hajo, and F. Kuppers, ''CW THz photomixers at 850 nm and 1550 nm using dielectrophoretic alignment of ag-nanowire,'' in *Proc. 41st Int. Conf. Infr., Millim., THz waves (IRMMW-THz)*, Copenhagen, Denmark, Sep. 2016, pp. 1–2.

[38] S. Preu, G. H. Döhler, S. Malzer, L. J. Wang, and A. C. Gossard, ''Tunable, continuous-wave terahertz photomixer sources and applications,'' *J. Appl. Phys.*, vol. 109, no. 6, Mar. 2011, Art. no. 061301.

[39] O. Cojocari, N. Sobornytskyy, C. Weickhmann, R. Jakoby, A. Semenov, H. Hübers, R. Müller, and A. Hoehl, ''Quasi optical Schottky diode detectors for fast ultra-wideband detection,'' in *Proc. IEEE Int. Conf. Microw. Millim. Wave Technol. (ICMMT)*, Jun. 2016, pp. 52–53.

[40] M. Hoefle, K. Haehnsen, I. Oprea, O. Cojocari, A. Penirschke, and R. Jakoby, ''Compact and sensitive millimetre wave detectors based on low barrier Schottky diodes on impedance matched planar antennas,'' *J. Infr., Millim., THz Waves*, vol. 35, no. 11, pp. 891–908, Nov. 2014.

AHID S. HAJO (Member, IEEE) received the master's degree in physics from the Institute of Physics, Goethe University Frankfurt, in May 2014. He is currently pursuing the Ph.D. degree with the Institute of Microwave Engineering and Photonics (IMP). After the master's degree at the Department of the Ultrafast Spectroscopy and Terahertz Physics, he worked as an Early-Stage Researcher (ESR) in the same research group and then at the Department of Photonics and Optical Communications, IMP, Technical University of Darmstadt. In October 2020, he joined the Department of the Terahertz Devices and Systems Laboratory, IMP. His experience covers the areas of terahertz and nanotechnology for the manufacture of new semiconductor devices for THz sources and detectors. He has authored or coauthored more than 25 journal articles and published conference contributions as well as two patents. His current research interests include the field of nanowire based THz Schottky detectors, GaN-based THz Gunn sources, CNT-based THz detectors and sources, and CNT-based BioNEMS sensors for biomedical applications.

SASCHA PREU (Member, IEEE) received the Diploma and Ph.D. degrees *(summa cum laude)* in physics from Friedrich-Alexander Universität Erlangen-Nürnberg, Erlangen, Germany, in 2005 and 2009, respectively. From 2004 to 2010, he was with the Max Planck Institute for the Science of Light, Erlangen. From 2010 to 2011, he was with the Department of Materials and Physics, University of California at Santa Barbara, CA, USA. From 2011 to 2014, he worked as the Chair of applied physics with Universität Erlangen-Nürnberg. He is currently a Full Professor with the Department of Electrical Engineering and Information Technology, Technical University of Darmstadt, Germany, leading the Terahertz Devices and Systems Laboratory. He has authored or coauthored more than 110 journal articles and published conference contributions. His research interests include the development of semiconductor-based terahertz sources and detectors, including photomixers, photoconductors and field effect transistor rectifiers, and terahertz systems constructed thereof. He also works on the applications of terahertz radiation, in particular the characterization of novel terahertz components and materials. In 2017, he received the ERC Starting Grant for developing ultra-broadband and photonic terahertz signal analyzers.

LEONID KOCHKUROV received the M.S. degree in physics from Saratov State University, in 2012, and the Ph.D. degree in laser physics from Yuri Gagarin State Technical University of Saratov, in 2017. In 2012, he joined the Department of Instrument Engineering, Yuri Gagarin State Technical University of Saratov, where he worked as an Engineer, from 2012 to 2014. From 2014 to 2015, he was an Invited Research Fellow at the Aston Institute of Photonic Technologies, Birmingham, U.K. From 2018 to 2019, he joined the Department of Photonics and Optical Communications, Institute of Microwave Engineering and Photonics (IMP), Technical University of Darmstadt. He is currently an Assistant Professor with the Department of Radio-Electronics and Telecommunication. He has authored or coauthored more than 30 journal articles and published conference contributions. His research interests include semiconductor lasers, nonlinear optics and nonlinear dynamics of lasers, high-speed optical communications, terahertz sources, and fiber optics.

THOMAS KUSSEROW received the Ph.D. degree from the University of Kassel, Germany, in 2010. The topic was about ''periodic InP/air-gap structures for MEMS and nano-optical devices.'' He was previously working on holographic optical elements at the Institute for Light and Building Technology (ILB), Cologne, from 1999 to 2001, and the Institute for Nanostructure Technology and Analytics (INA), Kassel, since 2005. His research was about MEMS and photonic crystals. In 2014, he became an Assistant Professor at INA, heading the Nanophotonics Group. In 2018, he was temporary for two years at the Photonics and Optical Communication Group at the Institute for Microwave Engineering and Photonics (IMP), Technical University Darmstadt. His current research interests include optical properties of nanostructures, emission from surface modes, and tailoring material properties.

OKTAY YILMAZOGLU received the Dr.-Ing. and Habilitation degrees from the Institute of Microwave Engineering, Technical University of Darmstadt, Darmstadt, Germany, in 2004 and 2013, respectively. He worked on several projects where compound semiconductor materials and technologies were used to develop sensors and electric devices on the basis of GaAs, GaN, and ZnO as well as carbon nanotubes and graphene for applications in mechanical engineering and at high-frequency. He has 20 years of expertise in microelectronic devices and components. This includes the design, fabrication, and characterization of 3-D magnetic field sensors, pressure sensors, gas sensors, acceleration sensors, high-frequency diodes, and nanostructured field emission devices for high frequency generation. His work includes the experimental use of 1-D or 2-D materials, as well as the theoretical evaluation of related quantum size effects. He is currently working in the field of THz photomixers as well as CNT- and graphene-based field-emission devices for sensing, electron source and microwave applications. These resulted in several patents and numerous publications in internationally highly regarded magazines.